

Modelling, Control, And Power Management for A Grid-Integrated Photo Voltaic, Fuel Cell, And Wind Hybrid System

Sushil Kumar Bhoi, Deptt. of Electrical Engg., Govt. College of Engineering, Kalahandi, Bhawanipatna, India
Email: sushilkumarbhoi@gmail.com

Abstract

Power management in a grid-integrated power system consisting of distributed renewable energy sources is necessitated by ever-increasing energy consumption, the high production cost, the limited fossil fuel resource, and the worsening global environment. Wind and solar power generation are two of the most promising renewable power generation technologies. The growth of wind and photovoltaic (PV) power generation systems has exceeded the most optimistic levels of expectations. Fuel cells (FCs) also have great potential to be green power sources of the future because of the many merits they have, such as high efficiency and zero or low emission of pollutant gases. In this paper the modelling, control, and analysis of grid-connected PV power, a proton exchange membrane fuel cell (PEMFC), and a wind energy system (WES) connected through a common DC bus linked to an AC grid is discussed. In coordination with the PEMFC, the hybrid system's output power becomes controllable so that full utilization of PV and wind power takes place based on its availability and the DC bus voltage is maintained constant even at varying load conditions for the desired power sharing between the distributed generation (DG) sources, load, and the AC grid. The hybrid system is controlled through a combination of two proposed control modes, namely the DG control mode and grid control mode. The coordination of the power controller, voltage source converter controller, and load controller is such that the transition between the two control modes is done as smoothly as possible. Thus, the total DG power will be a combination of PV power, WES power, and power produced by the PEMFC. Any additional power if required up to the maximum loading will be supplied by grid. If the load exceeds its maximum value, then the load controller will carry out load shedding. The composite system is available for safe operation in on-grid as well as of-grid mode satisfying voltage and power balance constraints. Different modes of operation have been demonstrated to verify and validate the desired power management among the DG sources, load, and the grid. MATLAB/Simulink software was used for simulating the composite model.

1 Introduction

A large portion of electrical power is still generated using conventional energy sources such as coal and fossil fuels, which are being depleted rapidly. As a result, there is a need to find alternative methods to meet power supply and demand without relying on traditional generation. In the past, renewable energy sources like solar and wind were introduced with basic technology, which only resulted in power generation without effective management of the output. Over recent years, research and investments have focused on hybrid power systems, which aim to provide an optimal solution for integrating solar and wind energy sources.

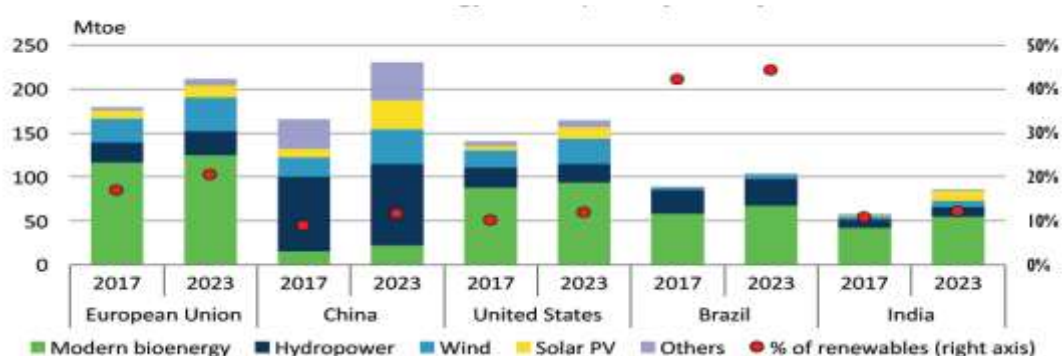


Figure 1. Renewable energy contribution to energy contribution by country from 2017-23

Hybrid systems, which combine renewable sources such as solar panels, wind turbines, and fuel cells, have gained importance as a way to produce clean and distributed energy. In parallel, the increasing use of distributed energy resources (DER), such as small-scale generators that harness renewable energy, is transforming how power systems operate. These

DERs reduce transmission losses and prevent grid congestion, especially in low-voltage distribution networks. Microgrids, small-scale systems of energy generation, are capable of operating independently during disturbances, ensuring reliable power supply.

2. Photovoltaic System & Its Modelling

2.1 Modelling of PV Panel

Usually, the equivalent circuit of a general PV model consists of a photocurrent, a diode, a parallel resistor which expresses a leakage current, and a series resistor which describes an internal resistance to the current flow as shown in fig 2. The voltage current characteristic equation of a solar cell is given as

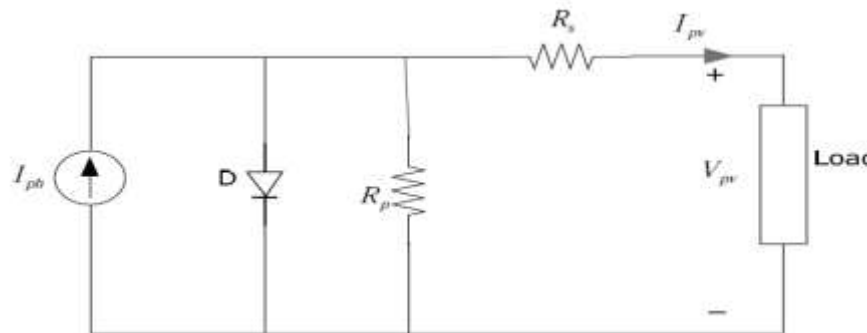


Figure 2. Equivalent circuit of a solar cell

$$I_{pv} = I_{ph} - I_s \left[\exp \left(q \frac{V_{pv} + I_{pv} R_s}{k T_c A} \right) - 1 \right] - \frac{V_{pv} + I_{pv} R_s}{R_p} \quad (1)$$

The photocurrent mainly depends on the cell's working temperature and solar irradiation, which is explained as

$$I_{ph} = \frac{[I_{sc} + K_i(T_c - T_{ref})] \lambda}{1000} \quad (2)$$

The saturation current of the cell varies with the cell temperature, which is represented as

$$I_s = I_{rs} \left(\frac{T_c}{T_{ref}} \right)^3 \exp \frac{[q E_g (\frac{1}{T_{ref}} - \frac{1}{T_c})]}{K_a} \quad (3)$$

The shunt resistance R_p of the cell is inversely related with shunt leakage current to the ground. Usually efficiency of PV array is insensitive to variation in R_p and the shunt-leakage resistance can be assumed to approach infinity without leakage current to ground.

Alternatively a small variation in series resistance R_s will significantly affect output power of the PV cell

$$I_{pv} = I_{ph} - I_s \left[\exp \frac{V_{pv} + I_{pv} R_s}{k T_c A} - 1 \right] \quad (4)$$

There is no series loss and no leakage to ground for an ideal PV cell, i.e., $R_s = 0$ and $R_p = \infty$.

$$I_{pv} = I_{ph} - I_s \left[\exp \frac{q V_{pv}}{k T_c A} - 1 \right] \quad (5)$$

A PV array is a group of several PV modules which are electrically connected in series and parallel circuits to generate the required current and voltage. So the current and voltage equation of the array with N_p parallel and N_s series cells can be represented as

$$I_{pv} = N_p I_{ph} - N_p I_s \left[\exp \left(q \frac{V_{pv} + I_{pv} R_s}{N_s k T_c A} \right) - 1 \right] - \frac{(N_p V_{pv} + I_{pv} R_s)}{R_p} \quad (6)$$

The efficiency of a PV cell is sensitive to small change in series resistance but insensitive to variation in shunt resistance. The role of series resistance is very important for a PV module and the shunt resistance is approached to be infinity which can also be assumed as open. The mathematical equation of the model can be described by considering series and parallel resistance as

$$I_{pv} = N_p I_{ph} - N_p I_s \left[\exp \frac{(q \frac{V_{pv} + I_{pv} R_s}{N_s})}{k T_c A} - 1 \right] \quad (7)$$

The above equation can be simplified as

$$I_{pv} = N_p I_{ph} - N_p I_s \left[\exp \left(\frac{q V_{pv}}{N_s k T_c A} \right) - 1 \right] \quad (8)$$

The open-circuit voltage V_{oc} and short-circuit current I_{sc} are the two most important parameters used which describes the cell electrical performance. The above mentioned equations are implicit and nonlinear; hence, it is not easy to arrive at an analytical solution for

the specific temperature and irradiance. Normally $I_{ph} \gg I_{sc}$ so by neglecting the small diode and ground-leakage currents under zero-terminal voltage, the short-circuit current is approximately equal to the photocurrent, i.e.

$$I_{ph} = I_{sc}$$

The open-circuit voltage parameter is obtained by assuming the zero output current. With the given open-circuit voltage at reference temperature and ignoring the shunt-leakage current, the reverse saturation current can be acquired as

$$I_{rs} = \frac{I_{sc}}{\exp\left(\frac{qV_{oc}}{N_s k T C_A}\right) - 1} \dots \dots \dots (9)$$

Additionally, the maximum power can be stated as

$$P_{max} = V_{max} * I_{max} = \gamma V_{oc} I_{sc} \dots \dots \dots (10)$$

3. Fuel Cell & Its Modelling

The electrochemical model of a fuel cell is based upon mathematical equations as referred to in [13]. The output voltage of a FC can be de need as:

$$V_{cell} = E_{cell} - V_{ohmic} - V_{act} \dots \dots \dots (11)$$

Where,

V_{cell} is the single fuel cell thermodynamic voltage,

V_{ohmic} is the ohmic voltage drop &

V_{act} is the cell activation voltage drop.

The thermodynamic voltage is calculated from the following Nernst equation

$$E_{cell} = 1.229 - 0.85 \cdot 10^{-3} (T_{cata} - 298.15) + \frac{R \cdot T_{cata}}{2F} \ln (\sqrt{P_{O_2cata}} \cdot PH_{2cata}) \dots (12)$$

The membrane resistance R_{mem} (Ω) is calculated by

$$R_{mem} = \frac{\int_0^{\delta_{mem}} r_{mem} dz}{A_{mem}} \dots \dots \dots (13)$$

Where, A_{mem} is the section surface of membrane (m^2), δ_{mem} is the membrane thickness (m). R_{mem} is the resistivity of membrane (Ωm) which can be calculated by the following equation.

$$r(mem) = \begin{cases} \frac{1}{0.1933} e^{[1268(\frac{1}{T_{mem}} - \frac{1}{303})]}, & \text{if } 0 < \lambda_w < 1 \\ \frac{1}{0.5193\lambda_w - 0.326} e^{[1268(\frac{1}{T_{mem}} - \frac{1}{303})]}, & \text{if } \lambda_w > 1 \end{cases} \dots \dots \dots (14)$$

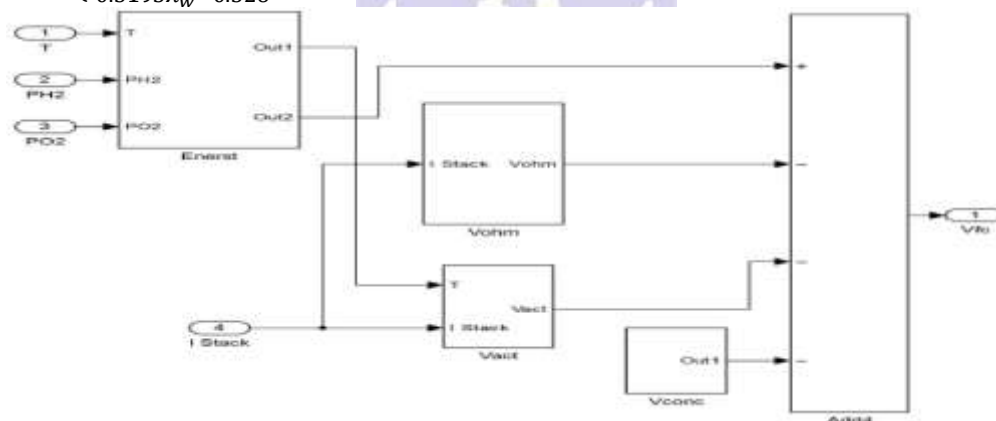


Figure 3. MATLAB simulation model of fuel cell



Figure 4. Output voltage of a fuel cell

The grid-integrated DG power system was suitably modeled and was simulated with MATLAB simulation software. The results are shown in Figure 29., which gives the output of the various renewable energy sources in the integrated DG system. In Figure 28, the first waveform corresponds to the power output of the PV system in kW. It can be seen that the output from a PV system varies with time starting with 58 kW to 78 kW, up to a maximum of 98 kW in a day.

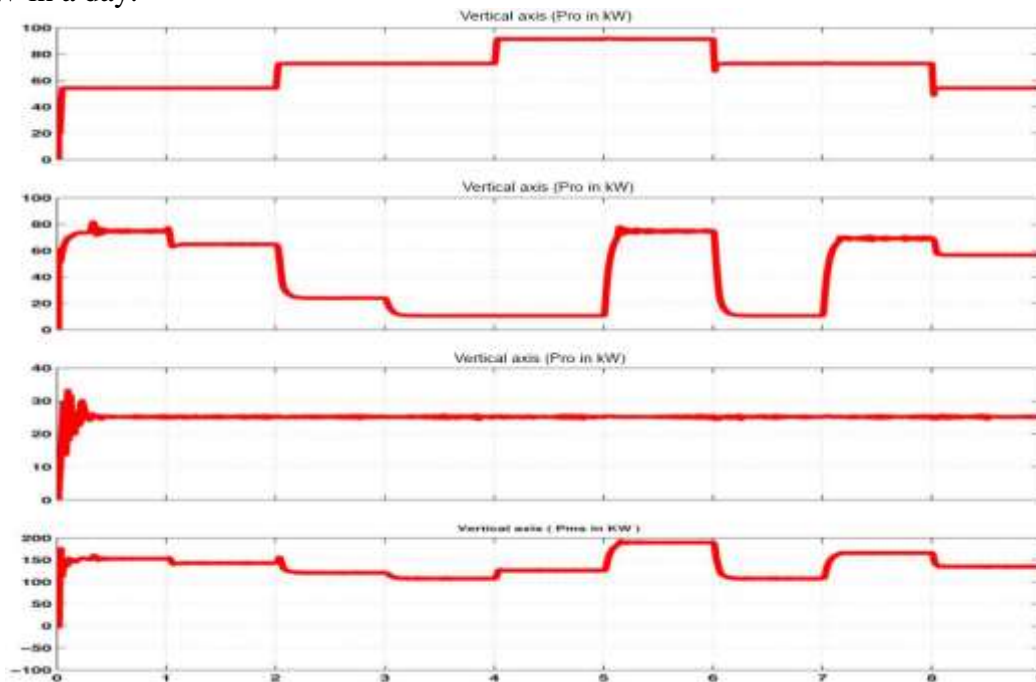


Figure 5. Output waveforms of PV, WES, and FC in kW

4.1 Waveforms depicting power flow from the sources, load, and grid

The waveforms in Figure 30. show the power levels at various points of the grid-integrated system. The first waveform is the consolidated power obtained from the renewable energy sources, namely the PV arrangement, WES, and FC. The second waveform shows the load demand in kW. The third waveform shows the support provided by the grid in order to maintain the load power at a constant. Thus, whenever there is a reduction in the renewable energy output the grid is connected to compensate. In Figure 6.2 the last waveform shows that the voltage across the load is regulated and remains constant. This method of control is called the grid-controlled method, as stated earlier.

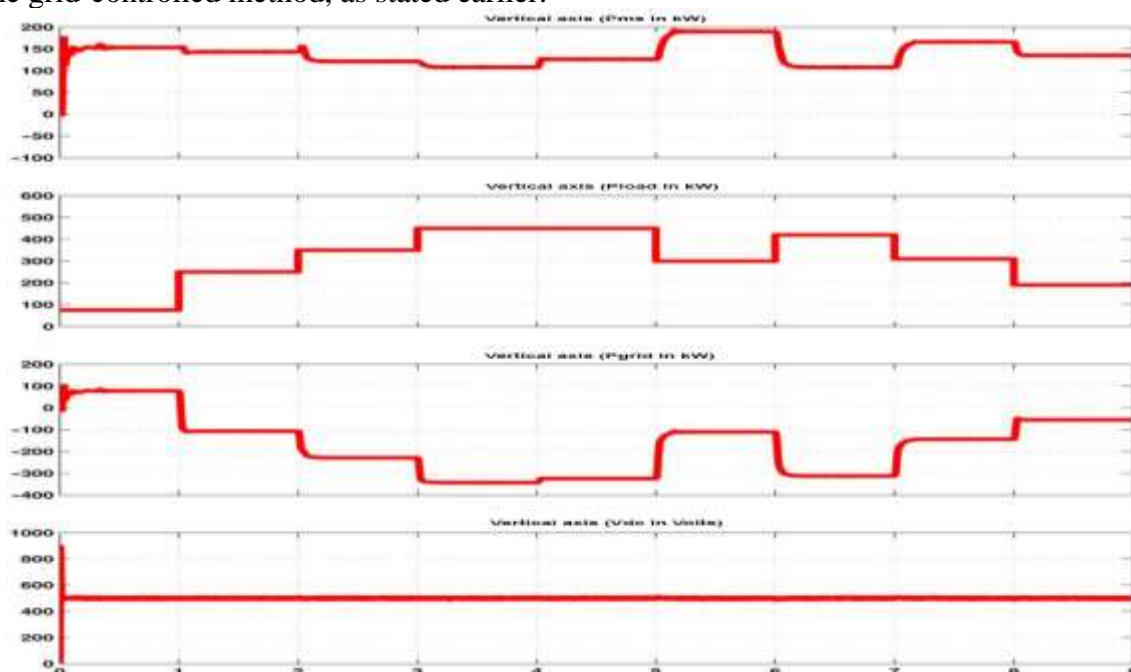


Figure 7. Waveforms depicting power flow from the sources, load, and grid.

4.2. Effect of controller on the DG output power

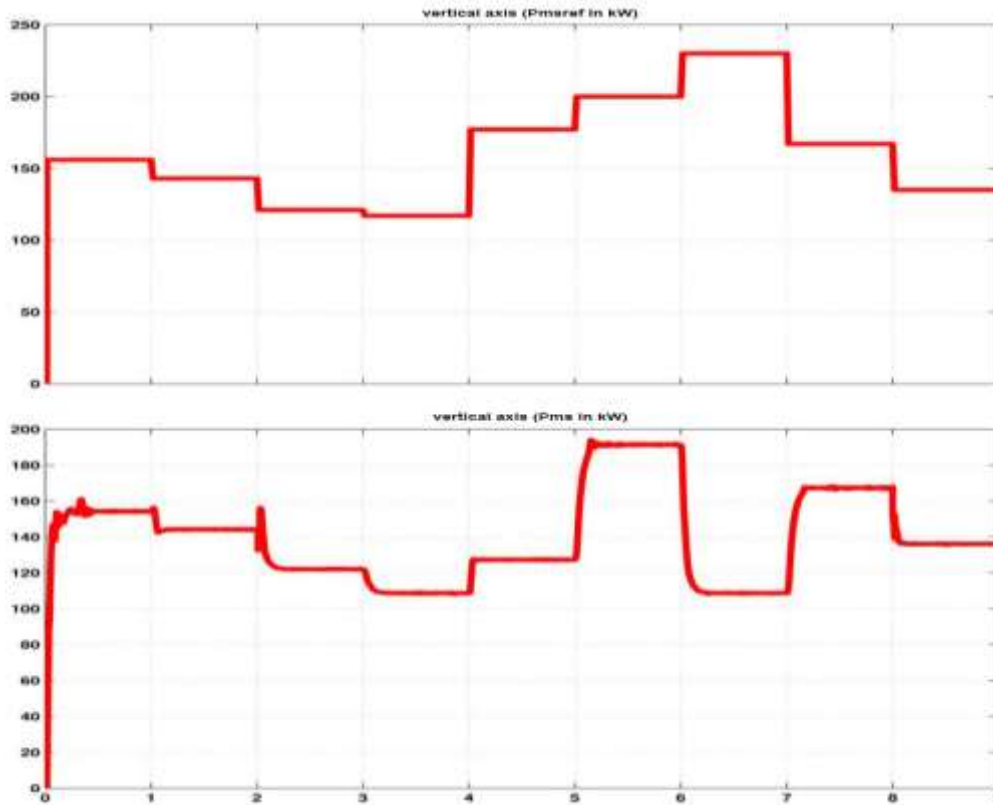


Figure 8. Effect of controller on the DG output

The effect of the control circuitry implemented in the grid-integrated distributed generation system is shown in Figure 31. It can be seen that the output of the DG system P_{ms} follows the reference P_{msref} . Thus, the controller plays an important role in maintaining the output power profile of the DG system.

4.3 Waveforms depicting load curtailment feature.

In contrast, Figure 32. shows what happens when the load demand is very high. Whenever the load is high there is a feature implemented in this grid-integrated DG system in which load shedding or load curtailment is automatically applied by the controller in order to match the DG generation and to provide grid independency. For the above, the loads that are not essentially necessary when there is a dip in the DG generation are identified and curtailment is applied while other critical loads are untouched. This ensures that the grid-integrated DG system acts similar to a microgrid.

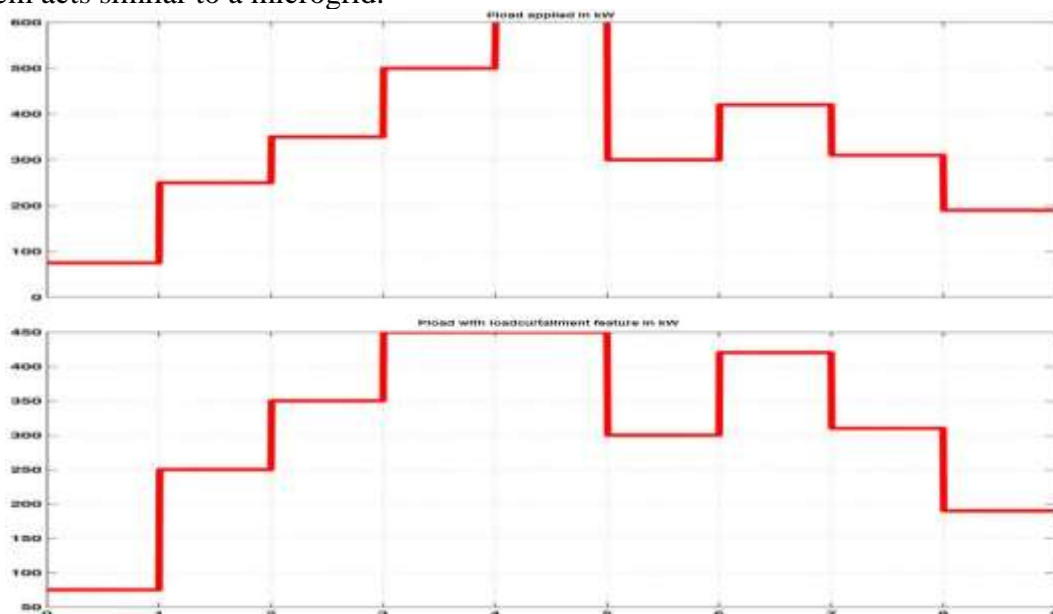


Figure 9. Waveforms depicting load curtailment feature

5.Conclusion

From the previous sections, it can be seen that the grid-integrated hybrid DG sources of PV-FC-WES operate satisfactorily as a combination of DGCM when the load is less than the renewable power generated and in GCM when the load is greater than the renewable generation. The load shedding is implemented as and when required. The DC bus voltage is maintained constant under all load conditions, satisfying the demand and supply balance, and hence power management between DG sources, load, and grid is achieved. The designed mathematical models and control strategies for PV, FC, WES, DC/DC converters, and inverter along with the power controller and load controller effectively achieve the smooth and satisfactory functioning of the grid-integrated hybrid system as mentioned above.

References

- [1] Yang H, Wei Z, Chengzh L. Optimal design and techno economic analysis of a hybrid solar-wind power generation system. *ApplEnergy* 2009; 86: 163-169.
- [2] Mahalakshmi M, Latha S. Modelling and simulation of solar photovoltaic wind and fuel cell hybrid energy systems. *Int J EngSci* 2012; 4: 2356-2365.
- [3] Wang C, Hashem NM. Power management of a stand-alone wind/photovoltaic/fuel cell energy system. *IEEE T Energy Conver* 2008; 23: 957-967.
- [4] Khanh LN, Jae JS, Kim YS. Power management strategies for a grid connected PV-FC hybrid system. *IEEE T Power Deliver* 2010; 25:1874-1882.
- [5] Katiraei I, Iravani MR. Power management strategies for a microgrid with multiple distributed generation units. *IEEE T Power Syst* 2006; 21: 1821-1831.
- [6] Lu ZX, Wang CX, Min Y. Overview on microgrid research. *Automation of Electric Power Systems* 2007; 31: 100-107.
- [7] Driesen J, Katiraei F. Design for distributed energy resources. *IEEE Power Energy M* 2008; 3: 30-40.
- [8] Rauschenbach HS, Solar Cell Array Design Handbook. New York, NY, USA: Van Nostrand Reinhold Co., 1980.
- [9] Ishaque K, Salam Z. An improved modelling method to determine the model parameters of photovoltaic modules using differential evaluation. *Sol Energy* 2011; 85: 2349-2359.
- [10] Villalva MG, Gazoli JR, Filho ER. Comprehensive approach to modelling and simulation of photovoltaic arrays. *IEEE T Power Electr* 2009; 24: 1198-1208.
- [11] Esram T, Chapman PL. Comparison of photovoltaic array maximum power point tracking techniques. *IEEE T Energy Conver* 2007; 22: 2183-2189.
- [12] Noguchi T, Togashi S, Nakamoto R. Short-current pulse-based maximum-power-point tracking method for multiple photovoltaic and converter module system. *IEEE T Ind Electron* 2002; 49: 217-223.
- [13] Jia J, Li Q, Wang Y, Cham Y T, Han M. Modelling and dynamic characteristics simulation of proton exchange membrane fuel cell. *IEEE T Energy Conver* 2009; 24: 2375-2381.
- [14] Hajizadeh A, Golkar MA. Intelligent power management strategy of hybrid distributed generation system. *Int J Elec Power* 2007; 29:783-795.
- [15] Leithead WE, Connor B. Control of variable speed wind turbines design task. *Int J Control* 2000; 13:1189-1212.
- [16] Garcia Hernandez R, Garduno Ramirez R. Modelling a wind turbine synchronous generator. *Int J Elec Power* 2013; 64-70.
- [17] Ramtharan G, Jenkins N. Modelling and control of synchronous generators for wide range variable speed wind turbines. *Wind Energy* 2007; 10: 231-246.
- [18] Chen Z, Spooner E. Grid power quality with variable speed wind turbines. *IEEE T Energy Conver* 2001; 16: 148-154.
- [19] Kim HW, Kim SS, Ko SS. Modelling and control of PMSG based variable speed wind turbine. *ElectrPowSyst Res* 2010; 80: 46-52.